



# Porous FeS<sub>2</sub> nanoparticles wrapped by reduced graphene oxide as high-performance Lithium-ion battery cathodes

Puqin Zhao<sup>a</sup>, Haohao Cui<sup>a</sup>, Jing Luan<sup>a</sup>, Zhengfeng Guo<sup>a</sup>, Yongxi Zhou<sup>b</sup>, Hongtao Xue<sup>b,\*</sup>

<sup>a</sup> Department of Applied Physics, Nanjing Technology University, Nanjing 210009, PR China

<sup>b</sup> College of Science, Department of Applied Physics, Advanced Energy Technology Center (AETC), Nanjing University of Posts and Telecommunications, Nanjing 210003, PR China

## ARTICLE INFO

### Keywords:

Porous materials  
Metallic composites  
Lithium-ion batteries

## ABSTRACT

Porous FeS<sub>2</sub> nanoparticles wrapped by reduced graphene oxide were synthesized by a facile one-step solvothermal approach and applied as cathode materials of Lithium-ion batteries. Porous structure and graphene help FeS<sub>2</sub> exhibits a superior cycling stability and rate performance, with a discharge capacity of 435 mA h g<sup>-1</sup> at a current density of 1000 mA g<sup>-1</sup> after 200 cycles. Moreover, the FeS<sub>2</sub> composite shows impressive performance at high current density. It retains a discharge capacity of over 170 mA h g<sup>-1</sup> even at a current density of 10 A g<sup>-1</sup> after 2000 cycles, demonstrating its potential applications as cathode materials for Lithium-ion batteries with high energy density.

## 1. Introduction

With the rapid development of future energy storage applications, high energy density and low-cost rechargeable Lithium-ion batteries (LIBs) are in high demand [1,2]. The pyrite FeS<sub>2</sub> has been investigated as an optical and electronic material for photovoltaic and energy storage applications due to their naturally abundance, inexpensive cost, high energy density and environmentally benign [3–6]. However, when used as the LIBs cathodes at room temperature, only limited rate performance and cycling stability has been achieved which is mainly due to the large effective electrical and interfacial resistance and the dissolution of polysulfide species [3–13].

Recently, research has focused on fabrication of novel FeS<sub>2</sub> as a cathode material in rechargeable LIBs [14–35]. Li et al. synthesized pyrite nanowire with a capacity of 350 mA h g<sup>-1</sup> after 50 cycles at a rate of 0.1 °C [14]. Yersak et al. reported a solid-state battery architecture which deliver a theoretical specific capacity of 890 mA h g<sup>-1</sup> at 60 °C [15]. Wu et al. demonstrated pyrite embedded carbon microspheres with a high capacity of 736 mA h g<sup>-1</sup> after 50 cycles at 50 mA g<sup>-1</sup> [16]. Son et al. made use of embedding natural pyrite in a polyacrylonitrile matrix with a capacity of 470 mA h g<sup>-1</sup> after 50 cycles at a rate of 0.1 °C [17]. Liu et al. increased FeS<sub>2</sub>@C porous nanooctahedra cathode with a capacity retention of 495 mA h g<sup>-1</sup> after 50 cycles at a rate of 0.5 °C [18]. Though the high capacities reported in these earlier studies clearly suggested that carbon-coated pyrite has good potential for LIBs applications, the capacity stability and rate performance of FeS<sub>2</sub>

cathode is still unsatisfying. Herein, we synthesized porous FeS<sub>2</sub> nanoparticles wrapped by reduced graphene oxide (*n*-FeS<sub>2</sub>/rGO) composite using a facile solvothermal approach. This composite exhibits comparatively high rate performance and superior cycling stability, demonstrating its potential applications for LIBs cathode with long cycling life and high power density.

## 2. Results and discussion

The process and characterization related to synthesis are described in detail in [Supplementary information](#). Fig. 1(a) shows that the SEM image of porous FeS<sub>2</sub> nanoparticles (*n*-FeS<sub>2</sub>) with diameter of about 500 nm. The FeS<sub>2</sub> nanoparticles are wrapped well by the rGO sheets with a reduced porosity and diameter which may be the obstruction influence of graphene during the formation reaction, as shown in Fig. 1(b). The TEM image and HRTEM image further in Fig. 1(c), (d) show the microstructures of the *n*-FeS<sub>2</sub>/rGO composite. Fig. 1(e) shows the XRD diffraction patterns of *n*-FeS<sub>2</sub>/rGO and *m*-FeS<sub>2</sub>/rGO, respectively. The two samples exhibit similar XRD pattern, and all diffraction peaks for the two samples can be well indexed to FeS<sub>2</sub> (JCPDF 65-3321). The FeS<sub>2</sub> microspheres (*m*-FeS<sub>2</sub>) and *m*-FeS<sub>2</sub>/rGO composites were also synthesized as shown in Fig. S1, TEM and HRTEM images confirm the formation of solid particles..

Fig. 2a shows the representative CV curves of the *n*-FeS<sub>2</sub>/rGO composite at a scanning rate of 0.1 mV s<sup>-1</sup> between 0.8 and 3.0 V versus Li<sup>+</sup>/Li. Detailed mechanisms for reduction and oxidation of

\* Corresponding author.

E-mail addresses: [pqzhao@gmail.com](mailto:pqzhao@gmail.com) (P. Zhao), [xueht@njupt.edu.cn](mailto:xueht@njupt.edu.cn) (H. Xue).

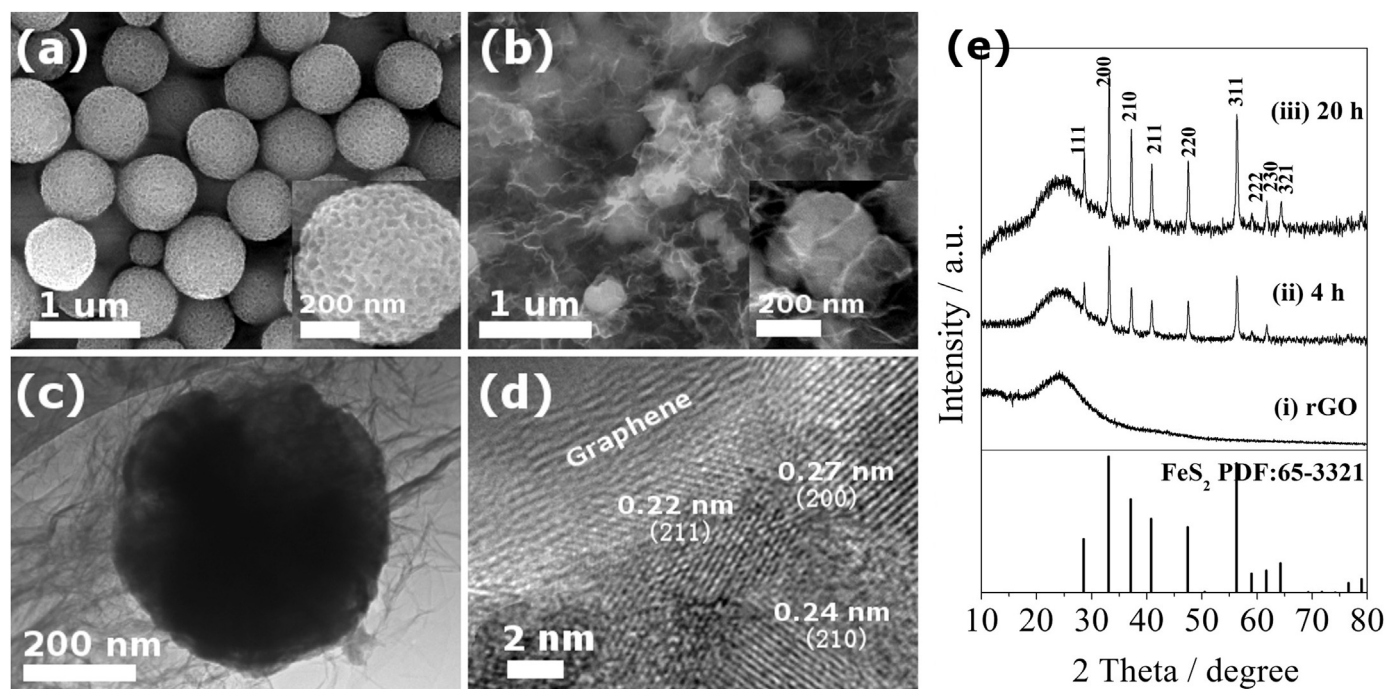


**Fig. 1.** (a) SEM image of porous  $\text{FeS}_2$  nanoparticles, (b, c, d) SEM, TEM and HRTEM images of  $n\text{-FeS}_2/\text{rGO}$  composite, (e) XRD patterns of (i) rGO, (ii) 4 h for  $n\text{-FeS}_2/\text{rGO}$  and (iii) 20 h for  $m\text{-FeS}_2/\text{rGO}$ .

lithium and  $\text{FeS}_2$  have been discussed in previous studies [12–16]. The first reduction peak at 1.2 V corresponds to the reaction of pyrite  $\text{FeS}_2$

lithiation:  $\text{FeS}_2 + 2\text{Li}^+ + 2\text{e}^- \rightarrow \text{Li}_2\text{FeS}_2$  and  $\text{Li}_2\text{FeS}_2 + 2\text{Li}^+ + 2\text{e}^- \rightarrow 2\text{Li}_2\text{S} + \text{Fe}$ . The two reactions proceed simultaneously as a single flat regime due to

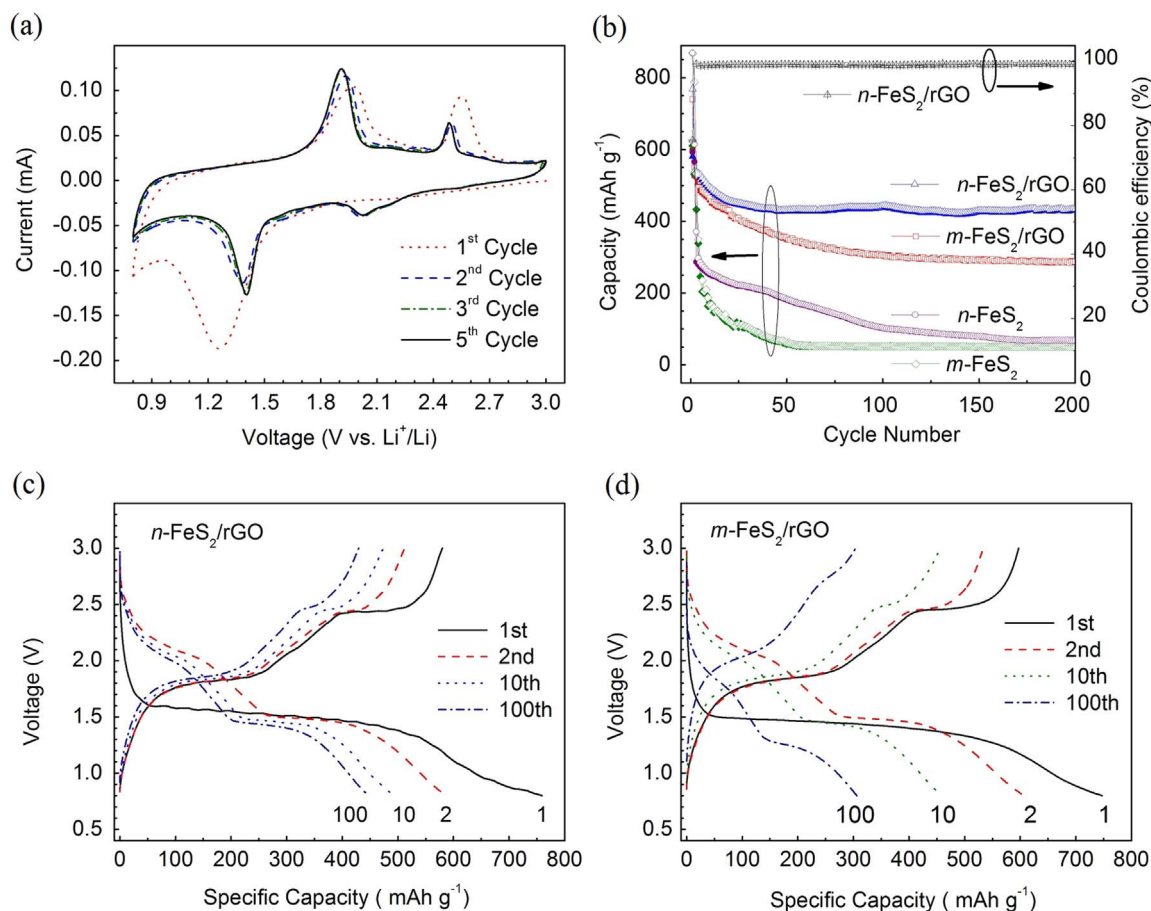


**Fig. 2.** Electrochemical Performance of  $n\text{-FeS}_2/\text{rGO}$  composite tested as cathode. (a) CV curves in the voltage range of 0.8–3.0 V with a sweep rate of  $0.1 \text{ mV s}^{-1}$ . (b) Cycling performances of  $n\text{-FeS}_2/\text{rGO}$ ,  $m\text{-FeS}_2/\text{rGO}$  and pure  $\text{FeS}_2$  particles at  $1000 \text{ mA g}^{-1}$ . Galvanostatic discharge/charge curves of (c)  $n\text{-FeS}_2/\text{rGO}$  and (d)  $m\text{-FeS}_2/\text{rGO}$  at  $1000 \text{ mA g}^{-1}$ .

Download English Version:

<https://daneshyari.com/en/article/5463683>

Download Persian Version:

<https://daneshyari.com/article/5463683>

[Daneshyari.com](https://daneshyari.com)